Aerosol Science and Technology, 39:40–51, 2005

ISSN: 0278-6826 print / 1521-7388 online
DOI: 10.1080/027868290901945

Evaluation of Multiangle Absorption Photometry for Measuring Aerosol Light Absorption

Andreas Petzold,[1] Herbert Schloesser,[2] Patrick J. Sheridan,[3] W. Patrick Arnott,[4] John A. Ogren,[3] and Aki Virkkula[5]

[1]*Institut für Physik der Atmosphäre, Deutsches Zentrum für Luft- und Raumfahrt Oberpfaffenhofen, Wessling, Germany*
[2]*Thermo ESM Andersen Instruments, Erlangen, Germany*
[3]*Climate Monitoring and Diagnostics Laboratory, National Oceanic and Atmospheric Administration, Boulder, Colorado, USA*
[4]*Desert Research Institute, Reno, Nevada, USA*
[5]*Finnish Meteorological Institute, Air Quality Research, Helsinki, Finland*

A new multiangle absorption photometer for the measurement of aerosol light absorption was recently introduced that builds on the simultaneous measurement of radiation transmitted through and scattered back from a particle-loaded fiber filter at multiple detection angles. The absorption coefficient of the filter-deposited aerosol is calculated from the optical properties of the entire filter system, which are determined by a two-stream-approximation radiative transfer scheme. In the course of the Reno Aerosol Optics Study (RAOS), the response characteristics of multiangle absorption photometry (MAAP) for white aerosol, pure black carbon aerosol from different sources, external mixtures of black and white aerosol, and ambient aerosol was investigated. The MAAP response characteristics were compared to basic filter transmittance and filter reflectance measurements. MAAP showed close agreement with a reference absorption measurement by extinction minus scattering. The slopes of regression lines vary between 0.99 ± 0.01 and 1.07 ± 0.02 for pure black carbon particles and external mixtures with ammonium sulphate to 1.03 ± 0.05 for ambient aerosol. No effect of the filter aerosol loading or the single-scattering albedo ω_0 of the sampled aerosol on the MAAP response characteristics was observed. In contrast, transmittance and reflectance methods showed a clear impact of ω_0 and the filter loading on the response characteristics, which requires the application of a correction function for the reliable determination of the aerosol absorption coefficient. In the case of nonabsorbing aerosol, the MAAP approach reduced the magnitude of the apparently measured absorption coefficient by one order of magnitude compared to a basic transmittance measurement.

INTRODUCTION

Measuring the aerosol absorption coefficient σ_{ap} is still a challenging task of high relevance. Besides in situ approaches such as photoacoustic spectroscopy (e.g., Petzold and Niessner 1996; Arnott et al. 2003) or the simultaneous measurement of aerosol extinction σ_{ep} and aerosol scattering σ_{sp} ($\sigma_{ap} = \sigma_{ep} - \sigma_{sp}$), one of the most frequently used approaches for aerosol absorption measurement is the collection of aerosol particles on a fiber filter matrix and the subsequent analysis of the sampled aerosol by optical means (see Horvath 1993 for an extensive overview). Two different instrumental setups are in wide use, and they both rely on the modification of the optical properties of a fiber filter matrix by deposited particles: filter transmittance measurements—e.g, the aethalometer (Hansen et al. 1984) and the particle soot absorption photometer (PSAP; Bond et al. 1999)—and filter reflectance measurements (e.g., Delumyea et al. 1980; Bailey and Clayton 1982). As was demonstrated in field studies (Liousse et al. 1993; Petzold et al. 1997), laboratory experiments (Bond et al. 1999; Weingartner et al. 2003), and model studies (Lindberg et al. 1999), the most frequently used filter transmission measurement method for the determination of the aerosol absorption coefficient shows a cross sensitivity to particle-related scattering effects and to multiple scattering effects caused by the filter matrix. Additionally, the impact of the filter aerosol loading on the measurement signal requires correction. Examples for the correction function for the filter transmittance method can be found, e.g., in Bond et al.

Received 23 January 2004; accepted 22 October 2004.
The support of Thermo Andersen for the operation of the MAAP Instrument during the Reno Aerosol Optics Study is acknowledged. The authors are grateful to an anonymous reviewer for helpful comments on the manuscript.
Address correspondence to Andreas Petzold, Institut für Physik der Atmosphäre, DLR Oberpfaffenhofen, D-82234 Wessling, Germany. E-mail: andreas.petzold@dlr.de

(1999) or in Weingartner et al. (2003). Thus, a simultaneous measurement of the aerosol scattering coefficient is required for data correction. This need for data correction is a serious limitation for filter transmittance methods.

A recently introduced method, the so-called multiangle absorption photometry (MAAP; Petzold et al. 2002; Petzold and Schönlinner 2004) combines simultaneous transmittance and reflectance measurements with the analysis of the particle-loaded filter by a two-stream-approximation radiative transfer scheme. The explicit treatment of light-scattering effects caused by the aerosol and by the filter matrix in the radiative transfer scheme is expected to improve the determination of the aerosol absorption coefficient by MAAP considerably. In the course of the Reno Aerosol Optics Study (RAOS), which put special emphasis on an intercomparison of in situ and filter-based methods for the measurement of the aerosol absorption coefficient (Sheridan et al. 2005), MAAP was for the first time extensively characterized and compared to several methods for the determination of σ_{ap}. The focus of this study is on the evaluation of the new MAAP method during the RAOS. Particularly, the response of MAAP to aerosols of different composition and optical properties were carefully investigated in order to prove or disprove the reduction of the method cross sensitivity to aerosol light-scattering effects by MAAP compared to basic methods filter transmittance and filter reflectance.

EXPERIMENTAL METHODS

The RAOS Design

During the RAOS, test aerosols of different composition and optical properties were generated and exposed to an extensive set of aerosol extinction, aerosol scattering, and aerosol absorption measurement methods. Sheridan et al. (2004) give a detailed overview over the RAOS approach and the obtained results. Briefly summarized, "white" ammonium sulphate particles and polystyrene latex spheres (PSL) were mixed with "black" combustion particles, which were generated with a kerosene burner and graphite particles emitted from a graphite vane pump. The mixing chamber was a 76 l stainless steel vessel. The single-scattering albedo $\omega_0 \equiv \sigma_{sp}/\sigma_{ep}$ of generated particle mixtures varied from about 0.30 for pure "black" aerosol, to 0.70–0.98 for externally mixed aerosols, and 1.0 for pure "white" aerosol. In addition to these test runs, measurements were performed with filtered particle-free air for testing the instruments' baseline behavior and with ambient aerosol.

As a reference method for the aerosol absorption measurement, aerosol extinction (σ_{ep}) measured with a folded-path optical extinction cell (Virkkula et al. 2005a) minus aerosol scattering (σ_{sp}) measured with a TSI 3563 integrating nephelometer was chosen, such that $\sigma_{ap} = \sigma_{ep} - \sigma_{sp}$. The absorption coefficient was also measured in situ by a photoacoustic spectrometer (Arnott et al. 2003). Deployed filter-based absorption measurement methods were a single-wavelength PSAP (Bond et al. 1999), one three-wavelength PSAP (Virkkula et al. 2005b), two multiple-wavelength aethalometers, and one single-wavelength MAAP. The adjustment between different wavelengths was obtained from multiple-wavelength measurements by interpolation (Sheridan et al. 2005).

Instrumental Setup

Multiangle Absorption Photometry. MAAP is based on a simultaneous measurement of radiation penetrating through and scattered back from a particle-loaded fiber filter. A detailed description of the method is given by Petzold and Schönlinner (2004). Figure 1 shows the arrangement of the light source and the detectors in the MAAP optical sensor (left) and the physical realization in the instrument (right). The physical background of the arrangement of detectors can be briefly summarized as follows: The measurement of the angular distribution of light scattered back and penetrated through a particle-loaded fiber filter showed that the radiation that has penetrated through the filter is completely diffuse and can be parameterized by a $\cos\theta$ relationship, with θ being the scattering angle relative to the incident radiation. The back-scattered radiation contains a diffusely scattered fraction proportional to $\cos(\theta - \pi)$, and a fraction that is parameterized best by a Gauss law proportional to $\exp[-1/2(\theta - \pi)^2/\rho^2]$, with ρ being a measure for the surface roughness of the aerosol layer deposited on the filter. The Gaussian-distributed fraction of the back-scattered radiation can be taken as radiation "reflected" from a rough surface. The partitioning of back-scattered radiation between diffuse and Gaussian type depends on the sampled aerosol. As is described in Petzold and Schönlinner (2004) in more detail, the measurement of the radiation penetrating through the filter at the scattering angle $\theta = 0$ deg, and the simultaneous measurement of the radiation scattered back from the filter at two detection angles $\theta = 130$ deg, and 165 deg, permits the full determination of the irradiances in the forward and back hemisphere relative to the incident light beam. The exact position of the detection angles was chosen such that the partitioning between diffuse and Gaussian types can be determined with highest resolution.

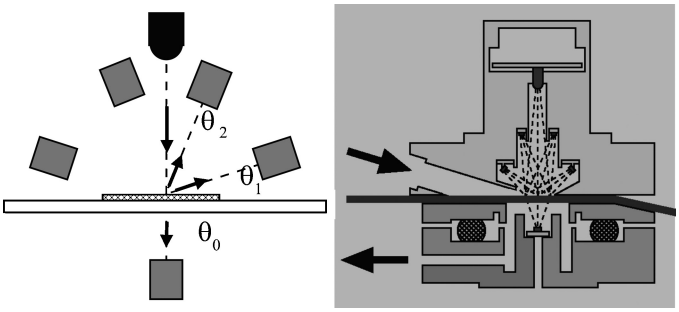

Figure 1. Optical sensor of the MAAP. Left: position of the photodetectors at detection angles $\theta_0 = 0^\circ$, $\theta_1 = 130^\circ$, and $\theta_2 = 165^\circ$ with respect to the incident light beam ($\lambda_{MAAP} = 670$ nm). Right: layout of the MAAP sensor unit, arrows indicate the airflow through the sensor unit across the filter tape.

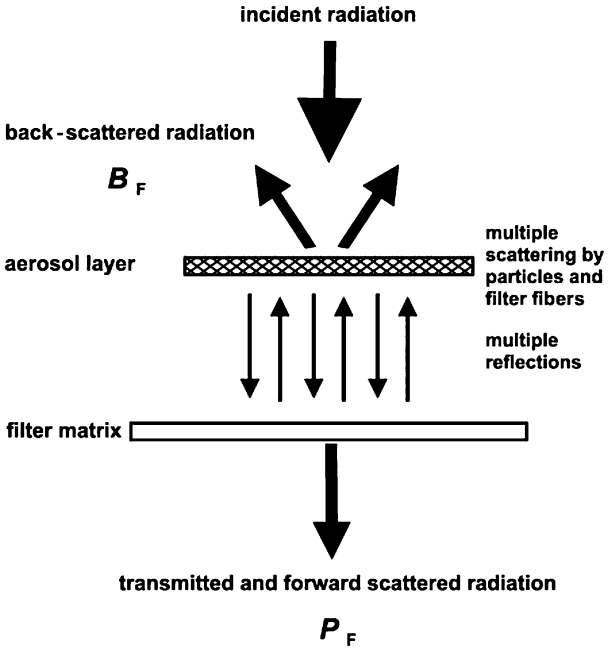

Figure 2. Schematic representation of radiation processes to be considered in the two-layer system consisting of an aerosol-loaded filter layer and the particle-free filter matrix.

In MAAP, the determination of the aerosol absorption coefficient of the deposited aerosol uses radiative transfer techniques. The particle-loaded filter is treated as a two-layer system: the aerosol-loaded layer of the filter and the particle-free filter matrix. Radiative processes inside the layer of deposited aerosol and between this layer and the particle-free filter matrix are taken separately into account. Figure 2 gives a schematic representation of important irradiances and interaction processes of the system. The treatment of radiative processes that are relevant in such a two-layer system has to consider the fraction of transmitted radiation T, the fraction of forward-scattered radiation F, the fraction of back-scattered radiation B, and the fraction of radiation penetrated through the particle-loaded filter P with $P = T + F$. The optical properties of the particle-free filter matrix (subscript M), the aerosol-loaded filter layer (subscript L), and the entire filter composed of the aerosol-loaded filter layer and the particle-free filter matrix (subscript F) have to be included. Diffuse (superscript *) and collimated (no superscript) incident radiation have to be distinguished.

In the applied approach which was originally developed by Hänel (1987) and modified for this purpose by Petzold and Schönlinner (2004), multiple reflections between the aerosol-loaded filter layer and the particle-free filter matrix are treated by the adding method (van de Hulst 1980). From this approach, the following budget equations for the ratio of radiation penetrating through a particle-loaded and a blank filter, $P_\mathrm{F}/P_\mathrm{F}^{(0)}$, and for the ratio of radiation scattered back from a particle-loaded and a blank filter, $B_\mathrm{F}/B_\mathrm{F}^{(0)}$, are obtained (Petzold and Schönlinner 2004):

$$\frac{P_\mathrm{F}}{P_\mathrm{F}^{(0)}} = \frac{T_L + F_L}{1 - B_L^* B_M}, \qquad [1a]$$

$$\frac{B_\mathrm{F}}{B_\mathrm{F}^{(0)}} = P_L^* \frac{T_L + F_L}{1 - B_L^* B_M} + \frac{B_L}{B_M}. \qquad [1b]$$

The filter properties $P_\mathrm{F}/P_\mathrm{F}^{(0)}$ and $B_\mathrm{F}/B_\mathrm{F}^{(0)}$ correspond to the ratios of penetrated and back-scattered radiation, respectively, for particle-loaded (P_F, B_F) and respective particle-free ($P_\mathrm{F}^{(0)}$, $B_\mathrm{F}^{(0)}$) filter samples. Establishing Equations (1a) and (1b) requires the approximation that the fraction of back-scattered radiation and the fraction of radiation penetrating through the filter are similar for the particle-free blank filter and the particle-free filter matrix of a particle-loaded filter, i.e., $P_\mathrm{F}^{(0)} \cong P_\mathrm{M}$, and $B_\mathrm{F}^{(0)} \cong B_\mathrm{M}$. These approximations are justified because the particles are deposited only in a very thin layer of the fiber filter, and the remaining particle-free part of the filter is almost as thick as the entire filter sample (Petzold and Schönlinner 2004). The term $(1–B_L^* B_\mathrm{M})$ describes the amplification of the irradiance by multiple reflections between the considered layers, while $T_\mathrm{L} + F_\mathrm{L}$ corresponds to the radiation passing through the aerosol-loaded filter layer; see also Figure 2 for more details.

The quantities $P_\mathrm{F}/P_\mathrm{F}^{(0)}$ and $B_\mathrm{F}/B_\mathrm{F}^{(0)}$ are directly measurable, while the properties F_L, B_L, P_L^*, and B_L^* of the aerosol-loaded filter layer have to be calculated via radiative transfer methods (Hänel 1987; Petzold and Schönlinner 2004). For treating the propagation of radiation through a system of light-scattering and light-absorbing components, the two-stream approximation for the equation of radiative transfer as proposed by Coakley and Chylek (1975) was used. The solution of the equation of radiative transfer (Hänel 1987; Petzold and Schönlinner 2004) yields equations for the quantities F_L, B_L, P_L^*, and B_L^* as functions of the ratio of light scattering to light extinction by the aerosol-loaded filter, which is the single-scattering albedo of the aerosol-loaded filter layer, $\mathrm{SSA_L}$.The missing filter matrix reflectivity was determined independently for the employed filter material as $B_\mathrm{M} \cong 0.70$.

The budget Equations (1a) and (1b) are solved in two steps. The properties F_L, B_L, P_L^*, and B_L^* are calculated from the two-stream approximation of the radiation transfer equation (Coakley and Chylek 1975; Haenel 1987) as a function of SSA_L. Then, the components of Equations (1a) and (1b) are calculated using the determined values F_L, B_L, P_L^*, and B_L^* and a starting value for the independent variable layer optical depth $\mathrm{LOD} = \ln T_\mathrm{L}$, which corresponds to the optical depth of the aerosol-loaded filter layer. The final solutions for the coupled Equations (1a) and (1b) are determined in an iterative process by varying the variables $\mathrm{SSA_L}$ and LOD, until both Equations (1a) and (1b) are simultaneously satisfied (Petzold and Schönlinner 2004).

It has to be noted that the properties LOD and $\mathrm{SSA_L}$ are mainly determined by the light-scattering characteristics of the

fibrous filter matrix. The contribution of light scattering to light extinction by the filter sample is obtained from the product LOD × SSA_L. However, a further separation into contributions of particles and filter fibers to light scattering by the particle-loaded filter cannot be given from the applied radiative transfer approximation method. In the case of light absorption, the situation is different, because the quartz or glass fibres do not contribute to light absorption in the spectral range selected for this instrument ($\lambda_{MAAP} = 670$ nm). The method-dependent coefficient $\sigma_{0\,(MAAP)}$ related to aerosol light absorption can thus be determined from the final values LOD and SSA_L as

$$\sigma_{0\,(MAAP)} = -\frac{A}{V}(1 - SSA_L)LOD. \qquad [2]$$

The property A refers to the active filter area, while V gives the sampled volume. The ratio A/V thus represents the inverse length of the aerosol column sampled through the filter spot. The final relation between $\sigma_{0\,(MAAP)}$ and the aerosol absorption coefficient σ_{ap} may require correction factors as discussed later.

The MAAP is set up in its current version as a continuously sampling instrument that uses a filter tape for aerosol sampling (see http://www.thermo.com/com/cda/product/detail/1,1055,19884,00.html for more information on the Thermo Model 5012 MAAP), and it is operated at a wavelength $\lambda_{MAAP} = 670$ nm. Standard operation conditions that were also used during RAOS are a sample flow of 1 m^3 h^{-1} and a time resolution of 2 min. Besides its original design feature for the simultaneous measurement of penetrating and back-scattered radiation, the optical sensor of the Model 5012 instrument offers the unique possibility of analyzing the recorded signals in terms of filter transmittance and filter reflectance separately from MAAP. As is demonstrated in Figure 3, MAAP uses all signals measured by the MAAP optical sensor unit, while filter transmittance (TRANS) and filter reflectance (REF) use only one detector signal. This important technical feature is used for the investigation of the sensitivity of MAAP and basic methods TRANS and REF to different types of black carbon aerosol and to effects of the filter aerosol loading and of the aerosol light-scattering component. Using the different MAAP signals for this kind of study compares method sensitivities to filter loading and aerosol properties for the same filter material and the same filter spot, which isolates method sensitivities from impacts of different filter media.

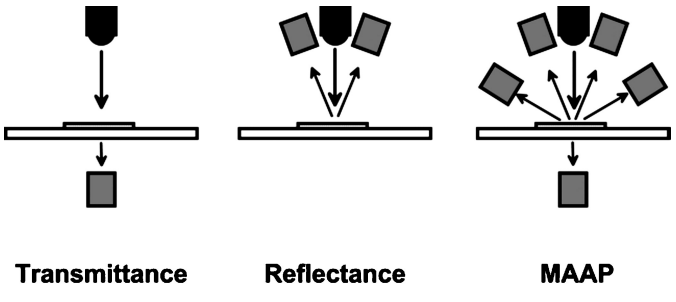

Figure 3. Principle measurement setups for different methods for the optical analysis of particle-loaded filters: filter transmittance (left), filter reflectance (mid), and MAAP (right).

Filter Transmittance and Reflectance. Basic TRANS and REF methods measure the change in filter transmittance or reflectance caused by the deposited aerosol particles. The filter transmittance T/T_0 (reflectance, R/R_0) of a filter sample is defined as the ratio of light intensities transmitted through or reflected from a particle-loaded and a particle-free filter, respectively. From these definitions, the method-dependent coefficients, $\sigma_{0\,(TRANS)}$ and $\sigma_{0\,(REF)}$, which describe the attenuation of light by the aerosol deposited on the investigated filter, are calculated as

$$\sigma_{0\,(TRANS)} = \frac{A}{V}\ln\left(\frac{T_0}{T}\right), \qquad [3a]$$

$$\sigma_{0\,(REF)} = \frac{1}{2}\frac{A}{V}\ln\left(\frac{R_0}{R}\right). \qquad [3b]$$

The factor $^1/_2$ in Equation (3b) compensates for the fact that in the case of a reflectance measurement the light beam passes the aerosol-loaded filter layer two times before measurement. Among the transmittance methods, the aethalometer (Hansen et al. 1984) and the particle soot absorption photometer (PSAP; Bond et al. 1999) are frequently used, while the reflectance method correspond to black smoke measurements (Bailey and Clayton 1982).

Correction Functions. There are two major artefacts that affect the measurement of aerosol optical properties from filter-deposited aerosol samples (e.g., Liousse et al. 1993; Petzold et al. 1997; Bond et al. 1999; Ballach et al. 2001; Weingartner et al. 2003; Arnott et al. 2005): (1) the influence of the aerosol loading of the filter sample on the measured absorption coefficient, and (2) an enhancement of the aerosol absorption coefficient caused by multiple scattering effects of the fibrous filter matrix and of the light-scattering aerosol components. In order to investigate the sensitivity of MAAP, transmittance measurement, and reflectance measurement to these artefacts, the correlation of the method-dependent coefficients $\sigma_{0\,(MAAP)}$, $\sigma_{0\,(TRANS)}$, and $\sigma_{0\,(REF)}$ with the aerosol absorption coefficient σ_{ap} was investigated separately for two types of black carbon particles (kerosene flame soot, graphite particles), for external mixtures of nonabsorbing ammonium sulphate and absorbing black carbon particles, and for ambient aerosol particles. From these data sets, the correction functions

$$\begin{aligned}
\sigma_{ap} &= \sigma_{0\,(MAAP)} f_{(MAAP)}(LOD) C_{(MAAP)}(\omega_0), \\
\sigma_{ap} &= \sigma_{0\,(TRANS)} f_{(TRANS)}(T/T_0) C_{(TRANS)}(\omega_0), \\
\sigma_{ap} &= \sigma_{0\,(REF)} f_{(REF)}(R/R_0) C_{(REF)}(\omega_0),
\end{aligned} \qquad [4]$$

were determined for each mode. The filter–matrix-dependent loading function f contains effects of the aerosol filter loading via the variables LOD, T/T_0, or R/R_0, respectively, while the function $C(\omega_0)$ contains effects of the aerosol-scattering component via the aerosol single-scattering albedo ω_0. The response

function is defined for all methods as the ratio between estimated absorption versus reference absorption,

$$\text{response function} \equiv \sigma_{0\,(\text{Method})}/\sigma_{\text{ap}}. \qquad [5]$$

From the method-dependent correction functions, an assessment of the impact of aerosol optical properties and filter-loading effects on the response of each investigated method will be given. This assessment of method sensitivities permits the final evaluation of MAAP in terms of the reduction of method cross sensitivities to effects of aerosol light scattering and filter loading. Although the achieved results hold only for the investigated type of fiber filter matrix, conclusions on the basic differences between the methods MAAP, TRANS, and REF can be drawn. It must be noted, however, that the details of the determined correction functions cannot be used for the correction of data obtained with other filter transmittance methods, because the correction functions depend strongly on the used filter matrix.

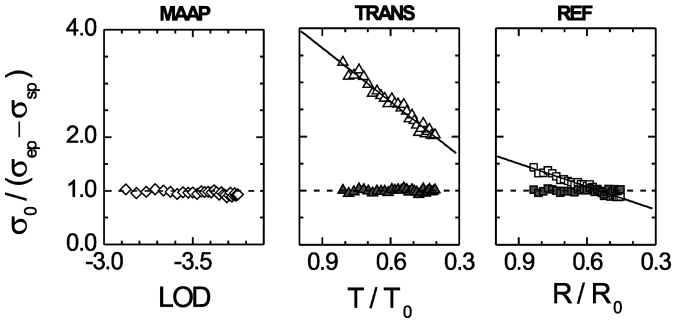

Figure 4. Response functions for methods MAAP, TRANS, and REF with respect to pure black carbon aerosol ($\omega_0 \cong 0.30$), solid lines represent the dependency of $\sigma_0/(\sigma_{\text{ep}}-\sigma_{\text{sp}})$ on the filter loading in units of layer optical depth LOD (MAAP), filter transmittance T/T_0 and filter reflectance R/R_0, respectively; dashed lines represent the line of equality, filled symbols correspond to data corrected for the filter loading effect.

RESULTS AND DISCUSSION

The results of the RAOS method evaluation are presented in a similar manner for all investigated methods. Method-dependent coefficients σ_0 were calculated for methods MAAP, TRANS, and REF according to Equations (2) and (3), and compared to the absorption coefficient σ_{ap}, measured with the reference method $\sigma_{\text{ap}} = \sigma_{\text{ep}} - \sigma_{\text{sp}}$ by linear regression analysis and by a statistical analysis of the ratio $\sigma_0/\sigma_{\text{ap}}$. All data sets are based on 2 min averaged data. This type of data analysis yields information on the relationship between in situ measured absorption coefficients and values measured by filter-based methods. Deviations can be attributed to artefacts in the σ_{ap} measurement, which are introduced by sampling the particles on the fibrous filter matrix.

Response Functions

According to Equation (5), a response function $\sigma_0/\sigma_{\text{ap}}$ that contains dependencies on the aerosol loading of the filter and on the light-scattering properties of the sampled aerosol is defined for all investigated methods. For an ideal instrument, the response function should be unity, i.e., $\sigma_0/\sigma_{\text{ap}} = 1$. The loading of the filter is defined as the difference in filter "blackness" between the blank white filter and the loaded filter. Measures for the filter loading are the layer optical depth (LOD) of the aerosol-loaded filter matrix for MAAP (see Equation (2) and explanations), filter transmittance, T/T_0, for transmittance measurements, and filter reflectance, R/R_0, for reflectance measurements, respectively. The respective loading values for a blank white filter are $\text{LOD}_0 \cong -2.54$, $T_0/T_0 = 1.0$, and $R_0/R_0 = 1.0$. All filter-loading measures decrease in magnitude with increasing filter loading. In order to compare the importance of this filter-loading effect for the various methods, the σ_0 values measured by each method were normalized to the reference value $\sigma_{\text{ap}} = \sigma_{\text{ep}} - \sigma_{\text{sp}}$ and plotted according to the loading value of the filter. For this analysis, only data from pure black aerosol samples were selected in order to separate the filter loading effect from the effect of light-scattering aerosol components.

Laboratory studies on filter transmittance methods (e.g., Bond et al. 1999; Weingartner et al. 2003; Arnott et al. 2004) have shown that the effect of the aerosol loading of the filter on the response of the method may have a serious impact on the σ_{ap}—values deduced from the measurements. Figure 4 and Table 1 summarize the respective results for pure black aerosol samples from kerosene flame particles obtained during RAOS. The filter-loading correction function is obtained from the parameters given in Table 1 via $f^{-1} = \text{a} + \text{m} \times \text{filter loading}$, following Equations (4). Filter transmittance and filter reflectance methods show a significant correlation between the filter loading and the method response in terms of $\sigma_0/\sigma_{\text{ap}}$ with $r^2 = 0.931$ to 0.938.

Table 1
Filter loading function f for MAAP, TRANS, and REF

	Kerosene soot		
n	30	30	30
r^2	0.179*	0.938	0.931
a	1.0	0.654 ± 0.066	0.226 ± 0.032
m	0.0	3.314 ± 0.113	1.415 ± 0.051
$\sigma_0/\sigma_{\text{ap}}$ (blank filter)	1.0	3.97	1.64
$\sigma_0/\sigma_{\text{ap}}$ (max. loaded filter)$^+$	1.0	1.98	0.86

*Correlation is not statistically significant.
$^+T/T_0$ (max.) = 0.40; R/R_0 (max.) = 0.45.
f is derived from pure kerosene soot data from the ratio $\sigma_0/\sigma_{\text{ap}}$ via $f^{-1} = \text{a} + \text{m} \times$ filter loading, following Equation (4).
The filter loading is given in units of layer optical depth LOD (MAAP), filter transmittance T/T_0 (TRANS), and filter reflectance R/R_0 (REF), respectively.
Parameters n and r^2 are number of data points and correlation coefficient.

In the case of MAAP, the correlation is not statistically significant ($r^2 = 0.179$). Figure 4 also contains transmittance and reflectance data corrected with the determined functions $f\,(T/T_0)$ and $f\,(R/R_0)$, displayed as filled symbols. The correction functions compensate the impact of the aerosol filter loading on the response $\sigma_0 \times f/\sigma_{ap}$ almost completely. The observed effect of the particle-loading of the filter on the response function σ_0/σ_{ap} is in good agreement with other studies on this effect concerning transmission measurement methods. Furthermore, the analysis of the aerosol-loaded fiber filter by radiative transfer techniques in the MAAP method seems to treat the multiple-scattering effects in the fibrous filter medium adequately, so that filter-loading corrections are no longer necessary.

Additional to the loading of the filter with absorbing aerosol, there exists also an influence of the aerosol single-scattering albedo ω_0 on the response factor σ_0/σ_{ap}, caused by additional multiple scattering of radiation in the aerosol-loaded filter layer. Figure 5 shows the response factors as a function of single-scattering albedo ω_0 without (top row panels) and with (bottom row panels) correcting for filter-loading effects. For both MAAP and the reflectance method REF, there is no significant relation between ω_0 and filter-loading corrected response ratios $\sigma_0 \times f/\sigma_{ap}$ observed. For the transmittance method TRANS, a significant increase of $\sigma_0 \times f/\sigma_{ap}$ with ω_0 is found that can be fitted by an exponential function. A comparable impact of the aerosol light-scattering coefficient on the measurement of the absorption coefficient is reported for the PSAP (Bond et al. 1999), which is also a transmittance measurement method. Respective correction functions for reflectance method are not available.

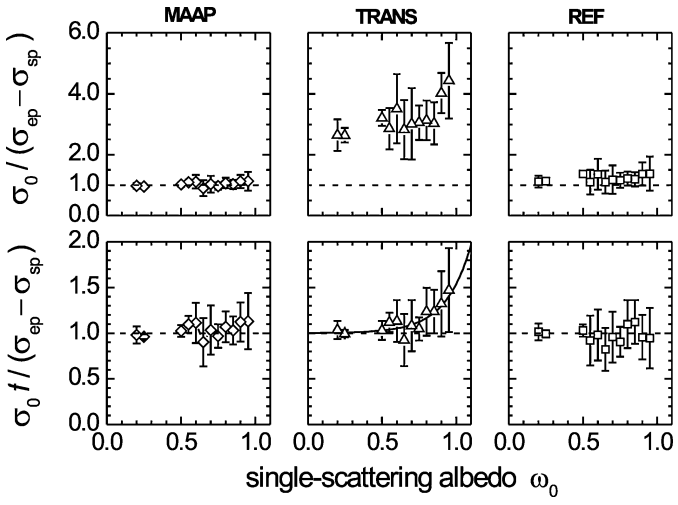

Figure 5. Response functions for methods MAAP, TRANS, and REF with respect to externally mixed grey and black aerosol of varying single-scattering albedo; top row panels show results without application of the filter loading correction function f, bottom row panels show respective results including the correction of the filter-loading effect; dashed lines represent the 1:1 ratio line, solid lines represent the single-scattering albedo response function $C(\omega_0)$.

Table 2
Method-specific correction functions for the conversion of measured coefficients, σ_0, into aerosol absorption coefficients, σ_{ap}

	MAAP	TRANS	REF
$f^{-1} =$	1.0	$0.654 + 3.314\frac{T}{T_0}$	$0.226 + 1.415\frac{R}{R_0}$
$C(\omega_0)^{-1} =$	1.0	$1.0 + 0.0015\exp(\frac{\omega_0}{0.17})$	1.0
$\sigma_{ap} =$	σ_0	$\sigma_0 \times f \times C(\omega_0)$	$\sigma_0 \times f$

Function f corrects for filter aerosol loading effect.
Function $C(\omega_0)$ corrects for effects of the aerosol single-scattering albedo ω_0.

From these data sets, the correction term $C(\omega_0)$ was derived for each method with the resulting parameter values given in Table 2. While MAAP data need no further correction procedures, the reflectance method values, $\sigma_{0(REF)}$ have to be corrected for the filter loading but do not require a correction for ω_0. The transmittance method values $\sigma_{0(TRANS)}$, however, require a correction for both filter loading and ω_0 effects. A summary of the full correction functions for all methods is compiled in Table 2 for particles emitted from a kerosene flame. Furthermore, the deviations of $\sigma_{0(MAAP)}$ values from reference σ_{ap} is almost independent of the magnitude of σ_{ap}, as is shown in Figure 6. The average difference $[\sigma_{0(MAAP)} - \sigma_{ap}]/\sigma_{ap}$ is of the order of 1.5%, with the standard deviation of the difference of 12% being in close agreement with the independently estimated method uncertainty of again 12% (Petzold and Schönlinner 2004).

An explanation for the different behavior of reflectance and transmittance measurement methods with respect to aerosol-scattering effects cannot be given from the radiative transfer approximation applied in MAAP. Studies concerning the physical processes behind these different behaviors require a radiative transfer model that is capable of separating the light-scattering contributions from particles and from filter fibers. Only with this type of model, a parameter study of the impact of aerosol single-scattering albedo ω_0 on the method response function σ_0/σ_{ap} is possible. Detailed investigations of this kind are beyond the scope of this study but will be subject of future research work.

Method Response to Aerosols of Various Composition

After having determined the correction functions for aerosol filter-loading effects and effects of multiple light-scattering processes, the response of the methods to aerosols of various compositions is investigated. The response of the investigated methods to externally mixed absorbing and nonabsorbing aerosols is shown in Figure 7 for ammonium sulphate–kerosene flame particles, and in Figure 8 for ammonium sulphate–graphite particles. Respective results from linear regression analyses and statistical analyses of the ratio σ_0/σ_{ap} are summarized in Table 3. The displayed unit for absorption coefficient data is $Mm^{-1} \equiv 10^{-6}\,m^{-1}$ in all graphs. The upper diagrams show raw data, while the lower

Table 3
Response of methods MAAP, TRANS, and REF to different types of pure black carbon and of black carbon mixed externally with ammonium sulphate

	Kerosene flame			Graphite particles		
	MAAP	TRANS	REF	MAAP	TRANS	REF
n	372	372	372	77	77	77
Raw data σ_0						
r^2	0.992	0.943	0.947	0.964	0.863	0.796
a	1.73 ± 0.59	17.23 ± 4.15	3.65 ± 1.85	-2.41 ± 0.85	17.40 ± 3.07	8.39 ± 2.05
m	0.99 ± 0.005	2.58 ± 0.03	1.10 ± 0.02	1.07 ± 0.02	1.86 ± 0.09	0.97 ± 0.06
m_{ZERO}	0.99 ± 0.01	2.65 ± 0.03	1.12 ± 0.01	1.01 ± 0.01	2.26 ± 0.06	1.16 ± 0.04
$\sigma_0/\sigma_{\mathrm{ap}}$	1.044 ± 0.357	3.330 ± 1.499	1.274 ± 0.547	0.944 ± 0.199	2.727 ± 0.681	1.361 ± 0.341
Corrected data $\sigma_0 \times f \times \mathrm{C}(\omega_0)$						
r^2	0.991	0.993	0.989	0.963	0.947	0.954
a	1.73 ± 0.59	-1.41 ± 0.64	-2.40 ± 0.77	-2.41 ± 0.85	-2.96 ± 0.87	-2.69 ± 1.04
m	0.99 ± 0.005	1.056 ± 0.005	1.050 ± 0.006	1.07 ± 0.02	0.88 ± 0.02	1.14 ± 0.03
m_{ZERO}	0.99 ± 0.01	1.05 ± 0.004	1.040 ± 0.005	1.01 ± 0.01	0.82 ± 0.01	1.07 ± 0.02
$\sigma_0/\sigma_{\mathrm{ap}}$	1.044 ± 0.357	1.035 ± 0.307	1.004 ± 0.342	0.944 ± 0.199	0.737 ± 0.156	1.002 ± 0.218

The response is given as $\sigma_{0\,(\mathrm{Method})} = a + m \times \sigma_{\mathrm{ap}}$, $\sigma_{0\,(\mathrm{Method})} = m_{\mathrm{ZERO}} \times \sigma_{\mathrm{ap}}$, and ratio $\sigma_{0\,(\mathrm{Method})}/\sigma_{\mathrm{ap}}$.
Independent variable is $\sigma_{\mathrm{ap}} \equiv \sigma_{\mathrm{ep}} - \sigma_{\mathrm{sp}}$.
Parameters n and r^2 are number of data points and correlation coefficient.
Top table reports results for raw data $\sigma_{0\,(\mathrm{Method})}$, bottom table reports respective results for corrected data $\sigma_0 \times f \times \mathrm{C}(\omega_0)$.

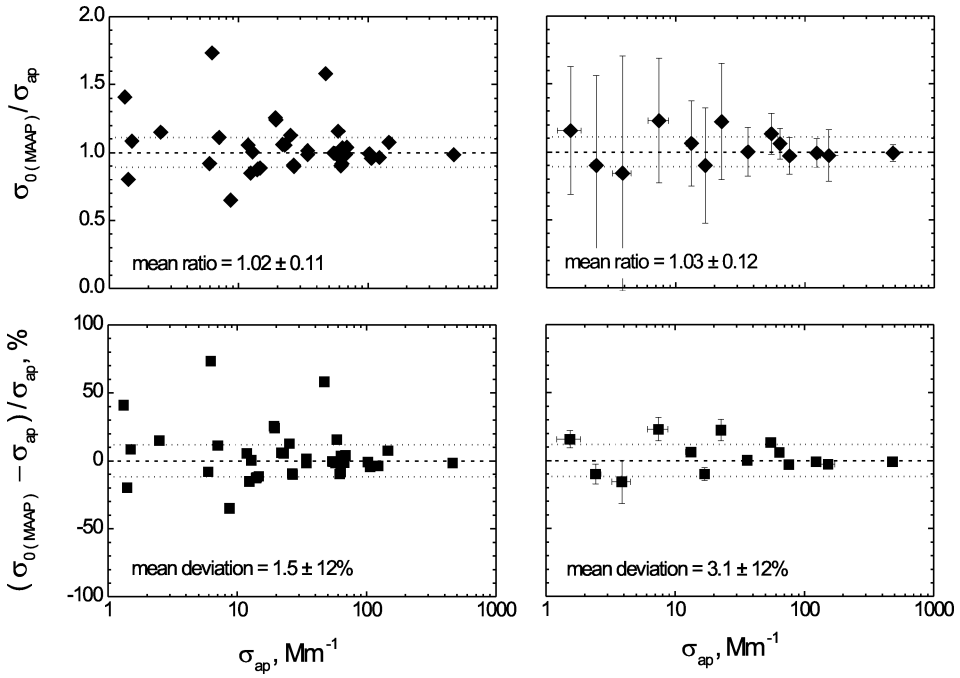

Figure 6. Ratio of raw MAAP data versus reference absorption data (top panels) and relative deviation of raw MAAP data from reference absorption data (bottom panels) as a function of the reference absorption coefficient σ_{ap}; the left (right) column shows results for run-averaged (2 min averaged) data. Dotted lines indicate the range $\pm$ one standard deviation.

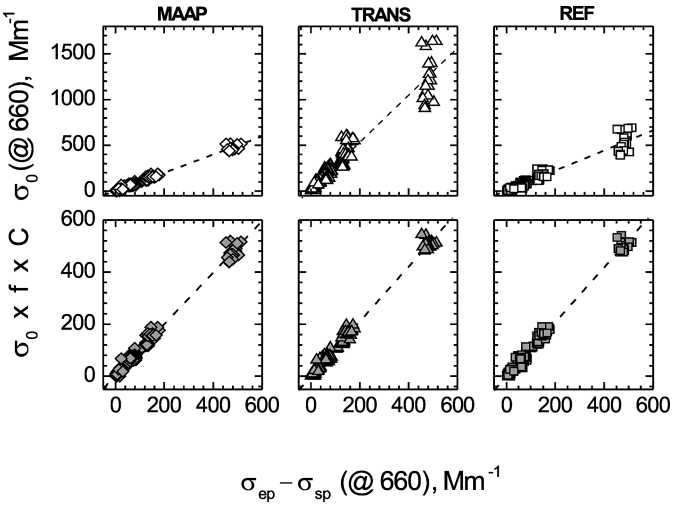

Figure 7. Method-dependent response coefficient σ_0 measured with MAAP, TRANS, and REF, respectively, as a function of the reference value $\sigma_{ap} = \sigma_{ep} - \sigma_{sp}$: externally mixed kerosene soot–ammonium sulphate aerosol; dashed lines give the linear regression lines. Top row panels represent uncorrected data σ_0, bottom row panels represent data corrected for filter-loading and aerosol-scattering effects $\sigma_0 \times f \times \mathrm{C}$.

diagrams present corrected data. All σ_0 values are highly correlated with the reference value σ_{ap}, independent of the selected method, with MAAP data showing the lowest scatter among all methods. For the MAAP method, the response to the two types

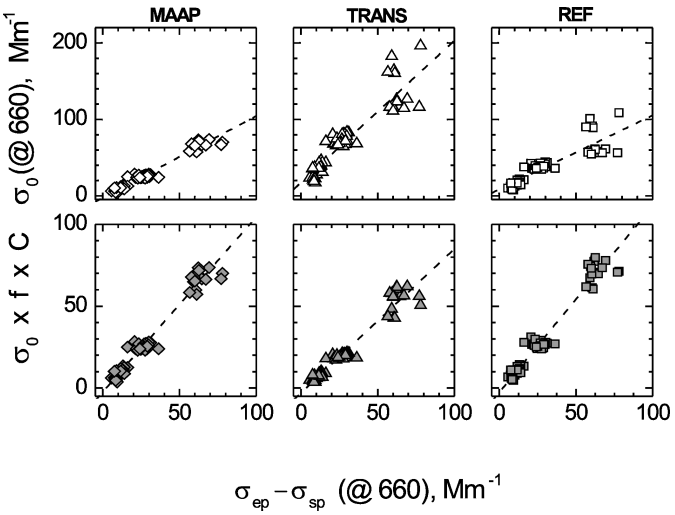

Figure 8. Method-dependent response coefficient σ_0 measured with MAAP, TRANS, and REF, respectively, as a function of the reference value $\sigma_{ap} = \sigma_{ep} - \sigma_{sp}$: externally mixed graphite soot–ammonium sulphate aerosol; dashed lines give the linear regression lines. Top row panels represent uncorrected data σ_0, bottom row panels represent data corrected for filter-loading and aerosol-scattering effects $\sigma_0 \times f \times \mathrm{C}$.

of black aerosol is almost identical with average ratios σ_0/σ_{ap} of 1.04 ± 0.36 and 0.94 ± 0.20 for kerosene flame particles and graphite particles, respectively, and slopes of regression lines in very good agreement with the average ratios σ_0/σ_{ap}.

Analyzing raw data, the transmittance method coefficients $\sigma_{0\,(\mathrm{TRANS})}$ exceed the reference value by a factor of 3.33 (kerosene flame) to 2.73 (graphite), which is a well-known behavior of the transmittance method (e.g., Bodhaine 1995; Weingartner et al. 2003; Arnott et al. 2005). In the case of the reflectance method, the deviations between σ_0 and σ_{ap} are weaker, but they are still significant. For raw data, a large scatter is found in the case of the transmittance method for high σ_{ap} values. A similar pattern of data scattering occurs in related PSAP data, as long as the effect of the aerosol-scattering coefficient is not properly corrected (Virkkula et al. 2005b). Since PSAP is a transmittance measurement method as well, this occurrence of similar data-scattering patterns is expected. For the reflectance method, a considerably weaker scatter of data is observed, while in the case of MAAP, no significant scatter of data is found.

Applying the determined correction functions for filter loading and aerosol light scattering, a close agreement between the measured absorption coefficients and the reference absorption coefficient $\sigma_{ap} = \sigma_{ep} - \sigma_{sp}$ is found for both filter transmittance and reflectance methods. The respective results are summarized in the bottom part of Table 3 and in the bottom panels of Figures 7 and 8. For the corrected data, all slopes of regression lines fall within an interval from 0.99 to 1.07 for kerosene flame particles, which justifies the developed correction functions. The comparability of properly corrected transmittance data, e.g., that originating from the PSAP (Virkkula et al. 2005b), and of data from in situ absorption measurement methods such as extinction minus scattering and photoacoustic spectroscopy, and of raw MAAP data, is demonstrated in Figure 9 and Table 4. Absorption

Table 4

Comparison of the MAAP to in situ methods and corrected PSAP for kerosene black carbon (pure and externally mixed with ammonium sulphate), given as $\sigma_{0\,(\mathrm{MAAP})} = a + m \times \sigma_{ap\,(\mathrm{Method})}$, $\sigma_{0\,(\mathrm{MAAP})} = m_{\mathrm{ZERO}} \times \sigma_{ap\,(\mathrm{Method})}$, and ratio $\sigma_{0\,(\mathrm{MAAP})}/\sigma_{ap\,(\mathrm{Method})}$

	Extinction Scattering	Photoacoustic	Corrected PSAP
n	449	421	488
r^2	0.992	0.929	0.992
a	1.39 ± 0.48	7.41 ± 1.48	1.65 ± 0.42
m	0.99 ± 0.004	0.89 ± 0.01	0.97 ± 0.004
m_{ZERO}	1.00 ± 0.004	0.92 ± 0.005	0.98 ± 0.003
$\sigma_{0\,(\mathrm{MAAP})}/\sigma_{ap}$	1.027 ± 0.337	1.190 ± 0.583	1.104 ± 0.242

Parameters n and r^2 are number of data points and correlation coefficient; all data refer to $\lambda = 660$ nm.

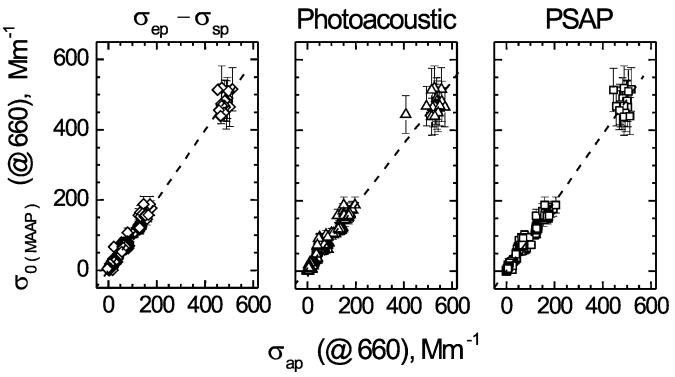

Figure 9. Method comparison of MAAP and reference method extinction–scattering, photoacoustic spectroscopy, and PSAP: externally mixed kerosene/graphite soot–ammonium sulphate aerosols, PSAP data are corrected for light-scattering and filter loading; dashed lines give the linear regression lines. Extinction–scattering, photoacoustic spectroscopy, and PSAP were operated at different wavelengths, adjustment to the MAAP wavelength of 660 nm was obtained by interpolation.

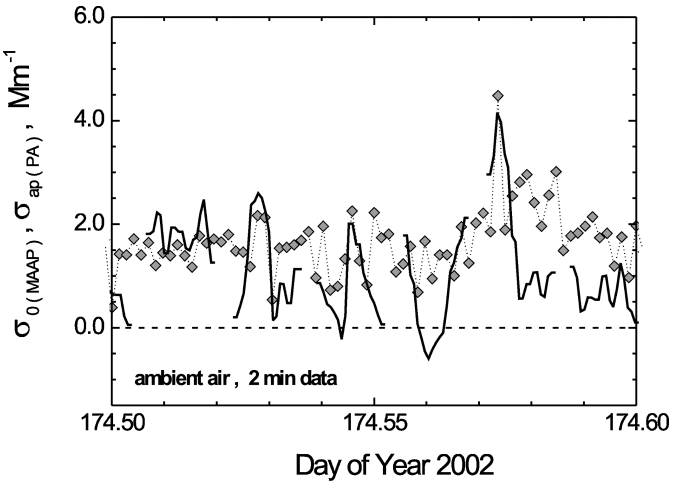

Figure 10. Time series of the MAAP response σ_0(diamonds) and the absorption coefficient σ_{ap} of ambient air aerosol measured with photoacoustic spectroscopy (solid line); data refer to $\lambda = 660$ nm.

coefficients measured by extinction minus scattering, MAAP, and corrected filter transmittance agree within an uncertainty of $\leq 11\%$ when the average ratios of absorption coefficients are considered. Photoacoustic spectroscopy, however, reports slightly lower absorption coefficients than MAAP, with the regression line showing a significant offset.

Sampling graphite particles, the slopes of regression lines extend from 0.88 to 1.14. The difference in response functions between graphite particles ($\sigma_0/\sigma_{ap} = 0.82$) and kerosene flame particles ($\sigma_0/\sigma_{ap} = 1.05$), e.g., for the transmittance method, may be caused by differing correction functions for the two types of black carbon particles, because in the MAAP data this difference does not occur. Unfortunately, the data base for graphite–ammonium sulphate mixtures is not sufficient for an appropriate determination of a graphite-related filter-loading correction function. Thus, the question of whether the correction function for filter reflectance and filter transmittance methods are transferable between different types of black carbon aerosol has to remain open for further research.

Investigations similar to those performed for externally mixed laboratory-generated particles were also conducted for ambient aerosol samples, which might be internally mixed to at least some degree. For that purpose, the instruments sampled ambient air for about 50 h during weekend conditions. An example of the measured $\sigma_{0\,(MAAP)}$ and σ_{ap} data is plotted in Figure 10. Ambient absorption coefficients were too low ($\sigma_{ap} < 4\ Mm^{-1}$) for the extinction cell, so that the photoacoustic instrument was taken as the in situ reference method. Measurements of the aerosol light-scattering coefficient were also not available for the ambient air measurements. Absorption coefficient data were converted from λ_{PA} to λ_{MAAP} by interpolation between the 532 nm and 1064 nm values of the photoacoustic spectrometer. As is demonstrated in Figure 10, both MAAP and the photoacoustic spectrometer data show similar patterns on a 2 min time base. However, the dynamic range of the MAAP instrument is reduced compared to the photoacoustic spectrometer. This reduction in the dynamic response to short-duration aerosol absorption peaks is caused by the fact that the photoacoustic spectrometer is a real-time and in situ instrument, while MAAP is in its current version only a quasi-real-time method because of the sampling interval of 2 min. However, this effect becomes important only for specific applications of monitoring highly variable absorption coefficients, but it can be neglected for long-term monitoring applications.

Linear regression analysis of ambient aerosol data was based on 60 min average data to partially compensate for the scatter of data introduced by the low absorption coefficient level in the ambient air. Respective results of the linear regression analysis are summarized in Figure 11 and Table 5. As for the laboratory aerosols, the upper diagrams show raw data, while the lower diagrams present corrected data. The same holds for the parameters summarized in Table 5. It has to be mentioned that for the ambient aerosol measurements only the filter loading was corrected, because aerosol light-scattering data were missing. Figure 11 shows clearly that the application of the loading correction alone does not improve the agreement between filter-based data and in situ data from the photoacoustic method, which is in contrast to the measurements using laboratory aerosols.

Response functions σ_0/σ_{ap} for the MAAP are in close agreement with the values found for laboratory-generated particles. The offset of MAAP data compared to photoacoustic data as found in the laboratory aerosol data occurs consistently in the ambient aerosol data and may be connected to photoacoustic-specific reasons (see also Arnott et al. 2003). Analyzing the filter loading corrected ratios $\sigma_0 \times f/\sigma_{ap}$ for the ambient aerosol data

Table 5

Response of MAAP, TRANS, and REF to ambient aerosol given as $\sigma_{0\,(\mathrm{Method})} = a + m \times \sigma_{\mathrm{ap\,(PA)}}$, $\sigma_{0\,(\mathrm{Method})} = \mathrm{m_{ZERO}} \times \sigma_{\mathrm{ap}}$, and ratio $\sigma_{0\,(\mathrm{Method})}/\sigma_{\mathrm{ap}}$, based on 1 h average data

	MAAP	TRANS	REF
n	47	47	47
Raw data σ_0			
r^2	0.564	0.487	0.429
a	0.49 ± 0.14	2.27 ± 0.61	0.81 ± 0.21
m	0.70 ± 0.10	2.93 ± 0.45	0.88 ± 0.15
m_{ZERO}	1.03 ± 0.05	4.44 ± 0.22	1.42 ± 0.08
$\sigma_0/\sigma_{\mathrm{ap}}$	1.180 ± 0.409	5.139 ± 1.793	1.657 ± 0.604
Corrected data $\sigma_0 \times f$			
r^2	0.564	0.394	0.391
a	0.49 ± 0.14	0.72 ± 0.20	0.56 ± 0.14
m	0.70 ± 0.10	0.78 ± 0.14	0.55 ± 0.10
m_{ZERO}	1.03 ± 0.05	1.26 ± 0.07	0.93 ± 0.05
$\sigma_0 \times f/\sigma_{\mathrm{ap}}$	1.180 ± 0.409	1.478 ± 0.565	1.098 ± 0.409

Parameters n and r^2 are number of data points and correlation coefficient, independent variable is $\sigma_{\mathrm{ap\,(PA)}}$ measured by photoacoustic spectroscopy.

Top table reports results for raw data $\sigma_{0\,(\mathrm{Method})}$, bottom table reports respective results for corrected data $\sigma_0 \times f$, the correction function $C(\omega_0)$ was not applied because ω_0 data were missing.

yield again a close agreement within the range of uncertainty for the reflectance method data with reference σ_{ap} data, while the transmittance method data are increased by a factor of 1.48 compared to σ_{ap} (see the bottom part of Table 5 for details). This residual deviation of transmittance method data from aerosol absorption coefficient data can be interpreted by means of $C_{\mathrm{TRANS}}(\omega_0)$, indicating $\omega_0 > 0.95$ for the sampled ambient aerosol.

In summary, the validation experiments with black carbon particles of various origin and ambient aerosol particles demonstrate the applicability of MAAP to the measurement of σ_{ap} without the need for further data correction. The method is comparable to in situ methods like extinction minus scattering and photoacoustic spectroscopy, and to appropriately corrected filter transmittance and filter reflectance measurement methods.

Method Response to Nonabsorbing Samples

The sensitivity of the investigated methods to nonabsorbing white aerosol is shown in Figure 12. Method-dependent coefficients σ_0 are plotted as fractions of respective extinction coefficients for PSL spheres (top row) and ammonium sulphate particles (bottom row). It has to be noted that in case of a nonabsorbing aerosol, the measured coefficient σ_0 corresponds to an apparently measured absorption coefficient. There is no significant difference in the method response to the different transparent aerosols. For extinction coefficients close to the atmospheric level ($\sigma_{\mathrm{ep}} < 60\ \mathrm{Mm^{-1}}$), the coefficient σ_0 varies from 3% of σ_{ep} for MAAP to 16% of σ_{ep} for the transmittance method. MAAP reduces the apparently measured absorption in the case of a "white" aerosol by almost one order of magnitude compared to the conventional transmittance method, and by a factor of 3 compared to the reflectance method. The cross sensitivity decreases with increasing aerosol load of the sampled air.

The fluctuations of σ_0 values measured in particle-free air is shown in Figure 13 as a distribution of occurrence frequencies. The data refer to a sampling time of 2 min and a sampling volume of 0.0334 $\mathrm{m^3}$, respectively. Blank value fluctuations are 0.14 ± 0.46 for MAAP, 0.61 ± 1.51 for the transmittance method, and 0.33 ± 0.82 for the reflectance method.

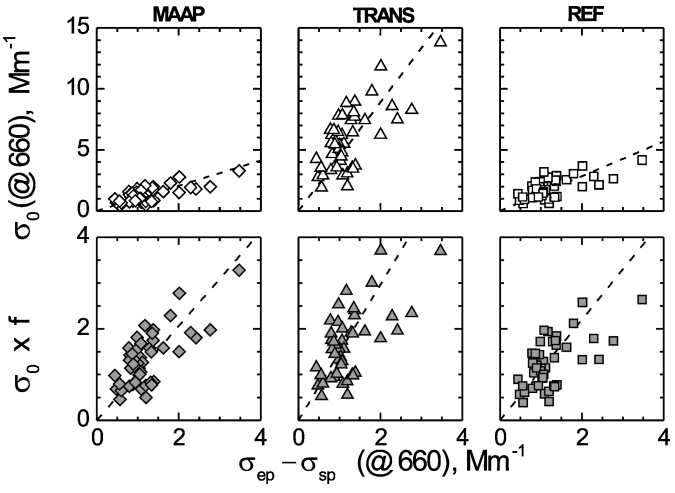

Figure 11. Method-dependent response coefficient σ_0 measured with MAAP, TRANS, and REF, respectively, as a function of the reference value σ_{ap} measured with photoacoustic spectroscopy: ambient aerosol, 60 min average data; dashed lines give the linear regression lines. Top row panels represent uncorrected data σ_0, bottom row panels represent data corrected for filter-loading effects $\sigma_0 \times f$.

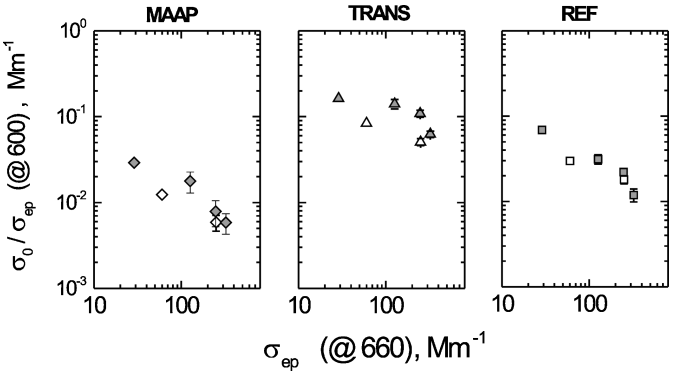

Figure 12. Method response to white aerosol displayed as ratio $\sigma_0/\sigma_{\mathrm{ep}}$: open symbols, PSL spheres; filled symbols, ammonium sulphate.

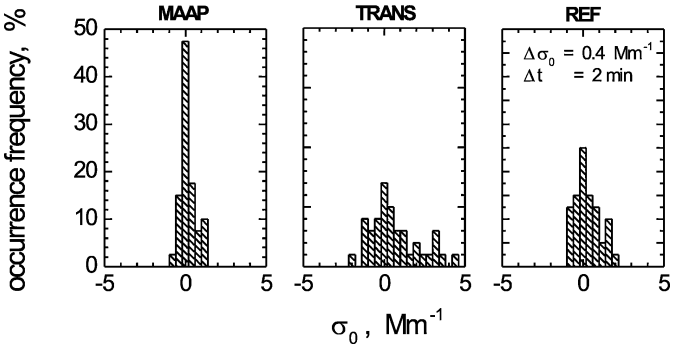

Figure 13. Response of methods MAAP, TRANS, and REF to filtered particle-free air, displayed as occurrence frequency distributions of apparent σ_{ap} values.

Resulting detection limits are 1.5 Mm^{-1} (MAAP), 5.1 Mm^{-1} (transmittance), and 2.8 Mm^{-1} (reflectance). In combination with the significant offset of the blank value fluctuations, the minimum detectable $\sigma_{0\,min\,(MAAP)}$ of 1.5 Mm^{-1} is reduced by a factor >3 compared to the transmittance method. While MAAP $\sigma_{0\,min}$ can be directly converted into a minimum detectable aerosol absorption coefficient $\sigma_{ap\,min}$, the values $\sigma_{0\,min}$ of the transmittance and reflectance methods have to be corrected for effects of filter loading and ω_0, which further reduces the performance of these modes compared to the MAAP method.

The detection limit in terms of σ_0 can be converted into a minimum resolvable filter absorbance ABS via Equation (2) by using $A = 2 \times 10^{-4}$ m^2 and $V = 0.0334$ m^3, yielding $ABS_{min} = 2.5 \times 10^{-4}$. Petzold and Schönlinner (2004) report a more conservative estimate from the variability of blank filter spot values of $ABS_{min} = 3.5 \times 10^{-4}$. Operating the MAAP at an averaging time of 1 h with the same sample flow will reduce the detection limit to 0.05–0.07 Mm^{-1}.

SUMMARY AND CONCLUSIONS

As part of the RAOS, an extensive evaluation of the recently introduced MAAP for the measurement of the aerosol absorption coefficient was conducted. Aerosols used during these evaluation experiments were two types of pure nonabsorbing particles, two types of absorbing black carbon particles, external mixtures of absorbing and nonabsorbing particles, and ambient particles. Additional to the evaluation of MAAP, filter transmittance and filter reflectance methods, which are both integral parts of the MAAP instrument, were simultaneously evaluated.

From all applied methods, only MAAP, which explicitly includes a treatment of scattering effects from the filter matrix and the light-scattering aerosol component, shows for all investigated aerosol types a 1:1 relationship to the reference absorption coefficient, which was inferred from extinction and scattering coefficient measurements. No difference between different types of black carbon particles was found. The observed range of deviations of MAAP absorption coefficient values from reference absorption coefficient values of 12% agrees with the independently estimated overall uncertainty of the new method.

Transmittance and reflectance methods require considerable corrections of the measured data before being converted into an aerosol absorption coefficient. While the reflectance method is found to depend only on the aerosol loading of the filter, the transmittance method also needs information on the aerosol single-scattering albedo for correction.

There are three major conclusions from this study:

1. MAAP is a new and promising approach for the measurement of the aerosol absorption coefficient by filter-based methods that requires no postmeasurement data correction or parallel-measured aerosol light-scattering coefficients.
2. Filter-based absorption measurement methods that do not include an adequate treatment of the effects of the filter matrix and the aerosol light-scattering component in the data analysis give wrong results caused by aerosol light-scattering processes and by the aerosol loading of the filter. The degree of perturbation of measured absorption coefficients is different for filter transmittance and filter reflectance methods.
3. If filter-based methods treat the perturbing effects properly, e.g., as by postmeasurement corrections using simultaneously measured light-scattering coefficients for PSAP data, or by considering these effects in the data analysis algorithm like MAAP does, filter-based approaches for aerosol absorption coefficient measurements are comparable to in situ methods with respect to a reliable σ_{ap}-measurement. Furthermore, filter-based methods for absorption coefficient measurement are able to measure σ_{ap}-values as low as 0.05 Mm^{-1} with a time resolution of 1 h as automated long-term monitoring instruments.

REFERENCES

Arnott, W. P., Moosmüller, H., Sheridan, P. J., Ogren, J. A., Raspet, R., Slaton, W. V., Hand, J. L., Kreidenweis, S. M., and Collett Jr., J. L. (2003). Photoacoustic and Filter-Based Ambient Aerosol Light Absorption Measurements: Instrument Comparisons and the Role of Relative Humidity, *J. Geophys. Res.* 108:AAC 15-1–AAC 15-11.

Arnott, W. P., Moosmüller, H., Sheridan, P. J., and Ogren, J. A. (2005). Evaluation of the Seven-Wavelength Aethalometer as an Aerosol Light Absorption Photometer, *Aerosol Sci. Technol.* 39:XXX–XXX.

Bailey, D. L. R., and Clayton, P. (1982). The Measurement of Suspended Particle and Total Carbon Concentration in the Atmosphere Using Standard Smoke Shade Methods, *Atmos. Environ.* 16:2683–2690.

Bodhaine, B. A. (1995). Aerosol Absorption Measurement at Barrow, Mauna Loa and the South Pole, *J. Geophys. Res*. 100:8967–8975.

Ballach, J., Hitzenberger, R., Schultz, E., and Jaeschke, W. (2001). Development of an Improved Optical Transmission Technique for Black Carbon (BC) Analysis, *Atmos. Environ.* 35:2089–2100.

Bond, T. C., Anderson, T. L., and Campbell, D. (1999). Calibration and Intercomparison of Filter-Based Measurements of Visible Light Absorption by Aerosols, *Aerosol Sci. Technol.* 30:582–600.

Coakley, J. A., and Chylek, P. (1975). The Two-Stream Approximation in Radiative Transfer: Including the Angle of Incident Radiation, *J. Atmos. Sci.* 32:409–418.

Delumyea, R. G., Chu, L.-C., and Macias, E. S. (1980). Determination of Elemental Carbon Component of Soot in Ambient Aerosol Samples, *Atmos. Env.* 14:647–652.

Hansen, A. D. A., Rosen, H., and Novakov, T. (1984). The Aethalometer—An Instrument for The Real-time Measurement of Optical Absorption by Aerosol Particles, *Sci. Total Envir.* 36:191–196.

Hänel, G. (1987). Radiation budget of the boundary layer: Part II, Simultaneous Measurement of Mean Solar Volume Absorption and Extinction Coefficients of Particles, *Beitr. Phys. Atmosph.* 60:241–247.

Horvath, H. (1993). Atmospheric Light Absorption, *Atmos. Environ.* 27A:293–317.

Lindberg, J. D., Douglass, R. E., and Garvey, D. M. (1999). Atmospheric Particulate Absorption and Black Carbon Measurement, *Appl. Opt.* 38:2369–2376.

Liousse, C., Cachier, H., and Jennings, S. G. (1993). Optical and Thermal Measurements of Black Carbon Aerosol Content in Different Environments: Variation of the Specific Attenuation Cross-Section, sigma (s), *Atmos. Environ.* 27A:1203–1211.

Petzold, A., Kopp, C., and Niessner, R. (1997). The Dependence of the Specific Attenuation Cross-Section on Black Carbon Mass Fraction and Particle Size, *Atmos. Environ.* 31:661–672.

Petzold, A., Kramer, H., and Schönlinner, M. (2002). Continuous Measurement of Atmospheric Black Carbon using a Multi-Angle Absorption Photometer, *Environ. Sci. Poll. Res.* 4:78–82.

Petzold, A., and Niessner, R. (1996). Photoacoustic Soot Sensor for In-Situ Black Carbon Monitoring, *Appl. Phys.* B 63:191–197.

Petzold, A., and Schönlinner, M. (2004). Multi-Angle Absorption Photometry—A New Method for the Measurement of Aerosol Light Absorption and Atmospheric Black Carbon, *J. Aerosol Sci.* in press.

Sheridan, P. J., Arnott, W. P., Ogren, J. A., Andrews, E., Atkinson, D. B., Covert, D. S., Moosmüller, H., Petzold, A., Schmidt, B., Strawa, A. W., Varma, R., and Virkkula, A. (2005). The Reno Aerosol Optics Study: Overview and Summary of Results, *Aerosol Sci. Technol.* 39:1–16.

van de Hulst, H. C. (1980). *Multiple Light Scattering* Vol I + II, Academic Press, New York.

Virkkula, A., Ahlquist, N., Covert, D., Sheridan, P., Arnott, W. P., and Ogren, J. (2005a). A Three-Wavelength Optical Extinction Cell for Measuring Aerosol Light Extinction and its Application to Determining Absorption Coefficient, *Aerosol Sci. Technol.* 39:52–67.

Virkkula, A., Ahlquist, N., Covert, D., Sheridan, P., Arnott, W. P., Sheridan, P. J., Quinn, P., and Coffman, D. (2005b). Modification, Calibration and a Field Test of an Instrument for Measuring Light Absorption by Particles, 2004b, *Aerosol Sci. Technol.* 39:68–83.

Weingartner, E., Saathoff, H., Schnaiter, M., Streit, N., Bitnar, B., and Baltensperger, U. (2003). Absorption of Light by Soot Particles: Determination of the Absorption Coefficient by Means of Aethalometers, *J. Aerosol Sci.* 34:1445–1463.